Local human activities overwhelm decreased sediment supply from the Changjiang River: Continued rapid accumulation in the Hangzhou Bay-Qiantang Estuary system

Xie, Dongfeng; Pan, Cunhong; Wu, Xiuguang; Gao, Shu; Wang, Zheng Bing

DOI
10.1016/j.margeo.2017.08.013

Publication date
2017

Document Version
Accepted author manuscript

Published in
Marine Geology

Citation (APA)
Xie, D., Pan, C., Wu, X., Gao, S., & Wang, Z. B. (2017). Local human activities overwhelm decreased sediment supply from the Changjiang River: Continued rapid accumulation in the Hangzhou Bay-Qiantang Estuary system. *Marine Geology*, *392*, 66-77. https://doi.org/10.1016/j.margeo.2017.08.013

Postprint of Marine Geology
Volume 392, 1 October 2017, Pages 66-77
Link to formal publication (Elsevier): https://doi.org/10.1016/j.margeo.2017.08.013

Local human activities overwhelm decreased sediment from the Changjiang River: continued rapid accumulation in the Hangzhou Bay-Qiantang Estuary system

Dongfeng Xie[a,*], Cunhong Pan[a], Xiuguang Wu[a], Shu Gao[b], Zhengbing Wang[c,d]

[a]Zhejiang Institute of Hydraulics and Estuary, Hangzhou, China.

[b]State Key Laboratory for Estuarine and Coastal Research, East China Normal University, Shanghai, China.

[c]Faculty of Civil Engineering and Geosciences, Delft University of Technology, The Netherlands.

[d]Deltares, P.O. Box 177, 2600 MH Delft, The Netherlands

*Corresponding author at: Zhejiang Institute of Hydraulics and Estuary, No.50 East Fengqi Road, Hangzhou, 310020, China.

E-mail address: dongfeng.xie@hotmail.com (D. Xie)

Abstract:

The aim of this contribution is to investigate the morphological responses of Hangzhou Bay, China, located immediately south of the Changjiang Estuary, to the drastic reduction of the sediment load from the Changjiang River and the large-scale coastal embankment over past decades. The spatial patterns of deposition and erosion, sediment volume changes, and the feedback with hydrodynamics and sediment transport were analyzed, on the basis of historical bathymetric and hydrographic data. The results show that the sedimentation rates in the bay have overall increased rather than decreased over the past decades, despite bed erosion having occurred in the northern bay-mouth. This reveals that the influence of the reduction in the Changjiang River sediment load on the

morphological evolution of Hangzhou Bay has to date been insignificant, mainly due to the buffering effect of existing sediment in the outer Changjiang Estuary. The morphological change is mainly related to the implementation process of the coastal embankment. Sediment accumulation induced by progressive seaward coastal embankment has resulted in seaward aggradation from the Qiantang Estuary towards Hangzhou Bay. Analysis of the annually-averaged high and low tidal levels, and durations of rising and falling tides reveals that flood dominance in the inner bay has been increased, due to the coastal embankment and sediment accumulation. The ratio between annually-averaged rising tide and falling tide durations have decreased from 0.85 to 0.63. The tidal prism at the interface between the inner and outer bay has decreased by about 25% since 1980s, while the net landward sediment flux has been intensified to a certain extent, which is responsible for the intensifying sedimentation in the inner bay. The local human activities have overcome the decreased sediment from the Changjiang River. Although the coastal embankment will cease in the near future, the morphological response to human activities is expected to continue on for a longer time.

Keywords: *Morphology; Sediment transport; Tidal asymmetry; Sediment load; Hangzhou Bay; Changjiang Estuary*.

1. Introduction

Estuaries are defined as semi-enclosed coastal bodies of water which have free connection with the open sea (Fairbridge, 1980). They are unique ecosystems and are often located in densely populated areas (e.g. Kennedy, 1984; Dyer, 1997; Trenhaile, 1997; Wang et al., 2015). River discharge, tidal currents, waves and sediment supply

48 are generally the major natural factors controlling the morphological evolution of
49 estuarine environments. On the other hand, morphodynamic development of an estuary
50 is also influenced by human activities such as flood protection, navigation channel
51 dredging, land reclamation, dam construction, or sand extraction. Such human activities
52 frequently cause substantial changes in the configuration of estuaries, their
53 hydrodynamic regime, sediment transport, deposition and erosion patterns (e.g. Van der
54 Wal et al., 2002; Blott et al., 2006; Wang et al., 2002, 2015; Winterwerp and Wang,
55 2013). In many cases the effects of human activities have exceeded changes induced by
56 natural forcing factors. From the coastal management point of view, it is of major
57 importance to understand the processes and mechanisms of morphological responses to
58 human activities and to predict the trends of their future evolution.
59
60 Worldwide, the transport rate of river-borne sediments into most estuaries has
61 apparently decreased in recent decades (Syviski et al., 2005; Milliman and Farnsworth,
62 2011). With the sediment supply reduction, rapid changes have taken place, among
63 them sediment transport adjustments, coastal retreat, slowdown of accumulation, and
64 even onset of erosion (e.g. Milliman, 1997; Syvitski et al., 2005; Yang et al., 2005,
65 2011; Gao and Wang, 2008). The Changjiang River is one of the largest rivers in the
66 world, ranking 3rd in length (6,400 km), 5th in runoff (925 km^3/y) and 4th in sediment
67 load (486 Mt/y) (Eisma, 1998). In the last 30 years, and especially since 2003 when the
68 Three Gorges Dam was constructed and operated, the sediment load at the Datong
69 measuring station located about 640 km upstream of the Changjiang River mouth (the
70 approximate limit of tidal penetration), has decreased drastically from more than 450
71 Mt/y before the1980s to less than 150 Mt/y, in some dry years (e.g. 2006 and 2011)

falling below 100 Mt (Fig. 1). As a result, the subaqueous delta of the Changjiang Estuary (CE) has switched from deposition to erosion, and the progradation rates of the fringing tidal flats have slowed down and locally even turned to degradation (Gao and Wang, 2008; Yang et al., 2011; Wang et al., 2015).

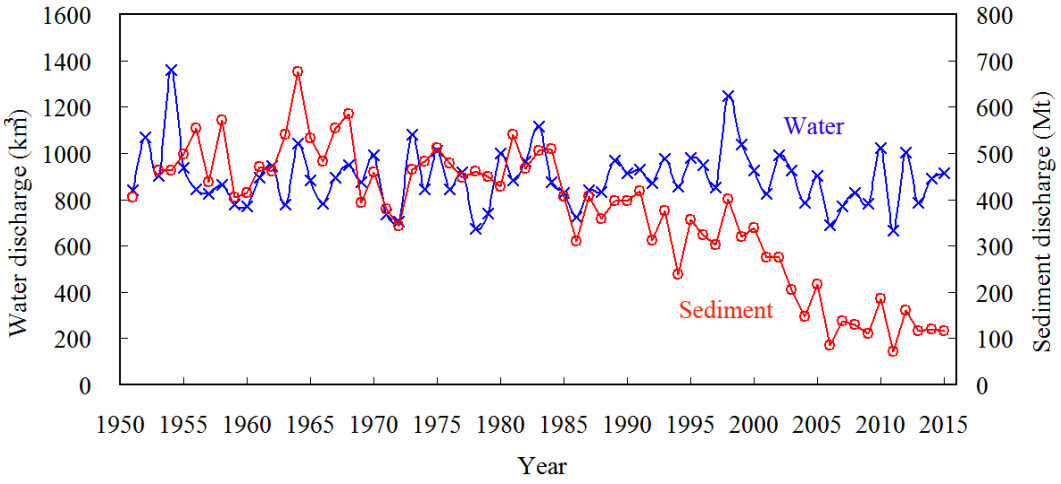

Fig. 1. Temporal variations of annual water and sediment discharges measured at the Datong gauging station located at the tidal limit 640 km upstream from the Changjiang River mouth (data from the Changjiang River Hydraulic Engineering Committee).

The Hangzhou Bay, located immediately south of the CE, is one of the largest embayment along the coast of the East China Sea, covering an area of about 4,800 km^2 (Fig. 2). Hangzhou Bay is typical funnel-shaped embayment and dominated by tidal currents. The west of Hangzhou Bay, from Ganpu to Zakou, is the Qiantang Estuary (QE), which is controlled by the combination of river discharge and tides (cf. Fig. 2). Hangzhou Bay is an area of extensive material exchange with the Changjiang Estuary, on one hand, and the Qiantang Estuary, on the other (e.g. Chen et al., 1990; Han et al., 2003).

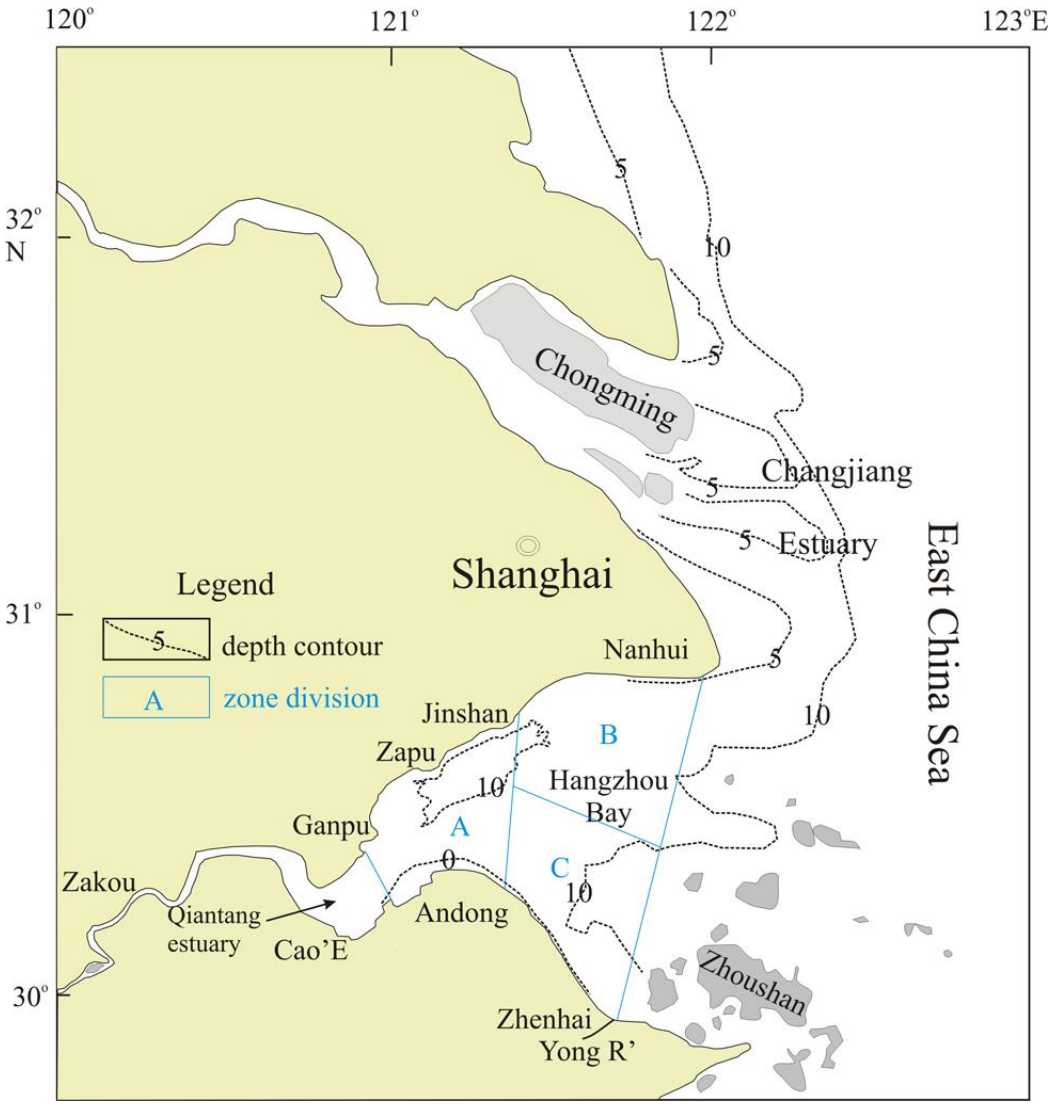

Fig. 2. Locations in Hangzhou Bay referred to in the text. The dashed lines depict water depths. The definitions of the three zones referred to in the statistics of Tables 1 are also given.

The recent drastic reduction of sediment discharge from the Changjiang River and its effect on the morphological evolution of Hangzhou Bay have been a matter of great concern to marine scientists, coastal engineers and the regional management. In recent years, the northern bay mouth has evolved from an accumulating area to an eroding area,

and thought to be related to reduction of sediment discharge from Changjiang River (e.g. Dai et al., 2014). However, little quantitative work has been done on the large-scale morphological response in Hangzhou Bay to such sediment reduction, in particular, on assessing whether the sediment input into Hangzhou Bay has decreased by taking the sediment exchange with the QE into account.

On the other hand, a large-scale coastal embankment program has been implemented in the QE since the 1960s (Fig. 3), aiming at improving flood protection and navigation (Li and Dai, 1986; Han et al., 2003; Pan et al., 2010). So far, more than 1000 km^2 of tidal flats have been reclaimed, substantially changing the configuration of the estuary. Li and Dai (1986) reported that sedimentation in the QE before the 1980s was mainly caused by the reduction of the tidal prism. They predicted qualitatively that, with the downstream constriction of the QE, accumulation would shift seaward and thereby cause the tidal prism to decrease further. Yu and Cao (2006) documented that sedimentation in the QE from the 1960s to 2000 amounted to about 250×10^6 m^3. The morphological response of the Hangzhou Bay to the embankments is expected to be slower than that of the QE. Recently, Yu et al. (2012) modeled the formation of the large longitudinal sand bar in the QE which elongated 130 km upward of Zapu and occupied the whole QE, using an idealized long-term 2-D model. Their model results showed the sandbar would shift seawards with the increasing convergence of the estuary, and erosion would occur first at the mouth area with the sediment supply decreasing at the sea side. However, their model results were not fully verified due to the lack of detailed information on the temporal evolution of the QE. Although numerous human activities take place concurrently in estuaries, morphologic responses have often been

observed to be slow (Wang et al., 2015). To capture the morphological evolution of the Hangzhou Bay, it is therefore necessary to base investigations on more and updated data.

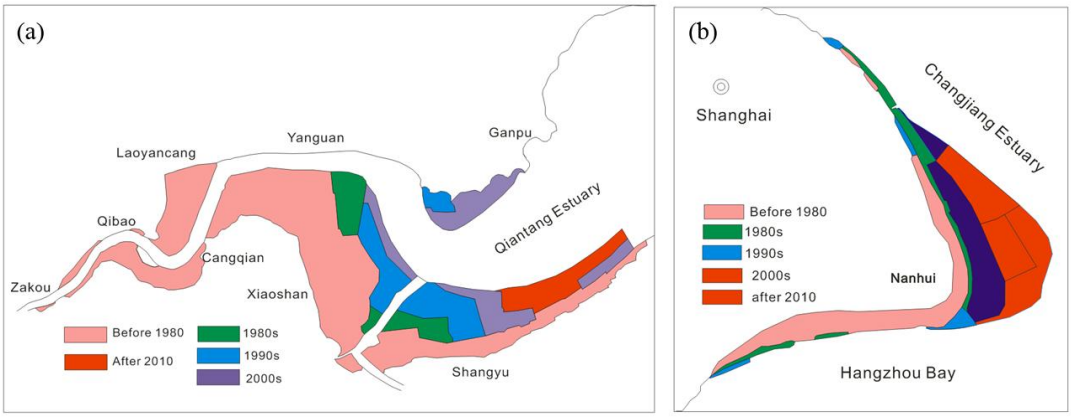

Fig. 3. Coastal embankment in the Qiantang Estuary (a) and land reclamations in front of the Nanhui flat bordering the Changjiang Estuary (b).

Short-term changes on more local scales can often be satisfactorily predicted using the so-called 'bottom-up' models, which are based on hydrodynamic models and other process-based computer models, but they have limited capabilities for the prediction of longer-term geomorphological evolution (e.g. Whitehouse, 2002; Townend and Whitehead, 2003). Hence, so-called 'top-down' models, which are based on historical trend analysis, are more frequently used (e.g. Wang et al., 2002; Van der Wal et al., 2002; Lane, 2004; Blott et al., 2006; Yang et al., 2011).

In this study, several detailed bathymetries of the Hangzhou Bay since 1959, long-term time series of channel volume data of the QE, as well as hydrographic data from representative stations have been compiled. On the basis of these data, deposition-

140 erosion patterns, sedimentation rates for different time intervals, and feedback between
141 hydrodynamics and morphological evolution have been reconstructed. In accordance,
142 the aims of the present study are to clarify whether the sediment supply to the Hangzhou
143 Bay has decreased since the drastic reduction in sediment discharge by the Changjiang
144 River, and to investigate whether any morphological responses are evident in the
145 Hangzhou Bay in response to the large-scale coastal embankments in the region.
146
147 **2. Regional setting**
148 The Hangzhou Bay is normally defined as the reach downstream of Ganpu to the
149 Nanhui-Zhenhai section at the bay mouth (Fig. 2). It is a typical funnel-shaped
150 embayment. The width at the mouth is about 98.5 km and decreases gradually to about
151 20 km some 100 km up-estuary. The total area of Hangzhou Bay amounts to about
152 4,800 km^2. The hydrodynamics and sediment transport are mainly controlled by tidal
153 currents in the bay. Upstream of the Hangzhou Bay, between the cities of Ganpu and
154 Zakou, is the 108 km long QE, which is controlled by the combination of river
155 discharges and tides.
156
157 The Hangzhou Bay can be divided into an outer and an inner part. The outer part from
158 the mouth to Jinshan covers an area of 3,000 km^2 (about 2/3 of the bay) is characterized
159 by a flat seabed with an average water depth of 8~10 m and incorporates numerous
160 scattered islands (Fig. 2). Upstream from Jinshan, the inner Hangzhou Bay covers an
161 area of 1,800 km^2 (about 1/3 of the bay). Between Zapu and the Qibao-Cangqian
162 section, the QE is occupied by a 130 km long, elongated subaqueous sandbar (Chien et
163 al., 1964; Han et al., 2003; Yu et al., 2012). Following the northern shoreline of the

middle part of the bay is a large, 60 km long and up to 50 m deep tidal channel, whereas the southern shore is lined by extensive tidal flats. As a whole, the morphology is characterized by sediment accumulation in the south and erosion in the north.

Runoff and sediment load of the Qiantang River are about 30 km^3/y and 3.40 Mt/y, respectively (Han et al., 2003). Runoff and sediment load of the Changjiang River are 925 km^3/y and 486 Mt/y, respectively, being ranked 5th and 4th in the world (Eisma, 1998). After the water and sediment enter the sea, one part is dispersed southward into the Hangzhou Bay due to the Changjiang secondary plume, representing the main sediment input to the Hangzhou Bay and the Qiantang Estuary (Su and Wang, 1989; Chen et al., 1990). With the sediment input from Changjiang Estuary, the average accumulation rate in the Hangzhou Bay used to be 1.15 cm/y (Xue, 1995). Despite the fact that the discharge of the Changjiang River has hardly changed over the last few decades, the sediment load has decreased continually since the 1980s, especially from 2003 onward when the Three Gorges Dam was constructed and operated (Fig. 1).

The semidiurnal tide is the main driving force behind the horizontal water flow in the Hangzhou Bay, with the M_2 constituent being the dominant tidal component (ECCHE, 1992). The tidal range is 2~4 m at the northern bay mouth, increasing upstream to reach a maximum at Ganpu with 4~6 m. At the southern mouth, the tidal range is only 1~2 m due to the sheltering effect of the Zhoushan archipelago. The deformation of the tidal wave is gradually enhanced upstream due to the progressive constriction of the estuary and the shoaling bathymetry along the large sandbar. This eventually evolves into be the world-famous, Qiantang tidal bore, with the maximum bore height over 3 m and the

188 maximum current velocity up to 5 m/s (Chen et al., 1990; Han et al., 2003; Pan and
189 Huang, 2010). In Hangzhou Bay tidal currents are strong, reaching maximum velocities
190 up to 3 m/s. The northern part is dominated by flood currents, whereas the southern part
191 is dominated by ebb currents. In correspondence, the residual flow and sediment
192 transport directions over one tidal cycle is landward in the north and seaward in the
193 south (Su and Wang, 1989; Xie et al., 2009).
194
195 Sediment in the Hangzhou Bay and the Qiantang Estuary is predominantly composed of
196 well sorted fine-grained non-cohesive silt, with the grain sized between 20 and 40 μm,
197 and transported in suspension (Fig. 4). Suspended sediments in the Hangzhou Bay are
198 vertically well-mixed. Suspended sediment concentration (SSC) in the bay is
199 characterized by three regions of high values separated by two of low values. Average
200 SSCs at the upstream end of the large sandbar, on the southern tidal flat and the
201 northeastern mouth region are 3.4~4.4, 1.2–~3.2 and 1.0~2.6 kg/m^3, respectively,
202 whereas in the southeastern bay and in the northern tidal channels the SSCs are less than
203 1.0 kg/m^3, respectively (Fig. 5). In the QE, the SSC can be more than 10 kg/m^3 at the
204 tidal bore arrival (Chen at al., 1990; Pan and Huang, 2010; Tu and Fan, 2017). Wind
205 generated waves in the bay reach heights of 0.2~0.5 m (ECCHE, 1992).

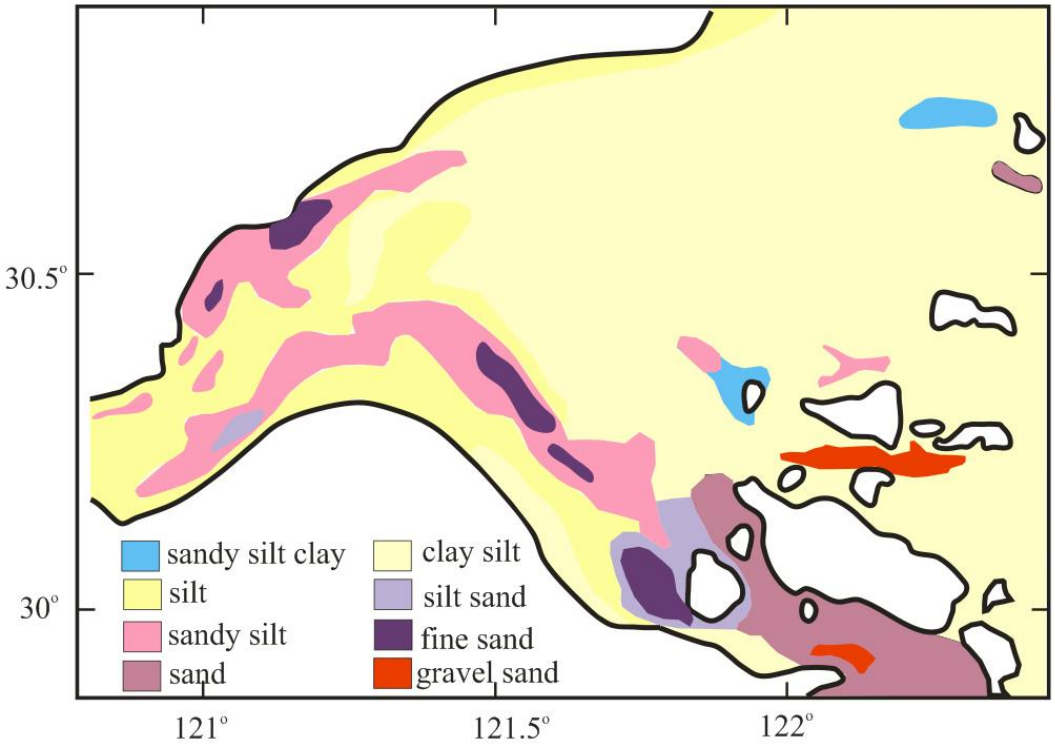

206
207 Fig. 4. Surface sediment grain size in Hangzhou Bay (from Xie et al., 2009).

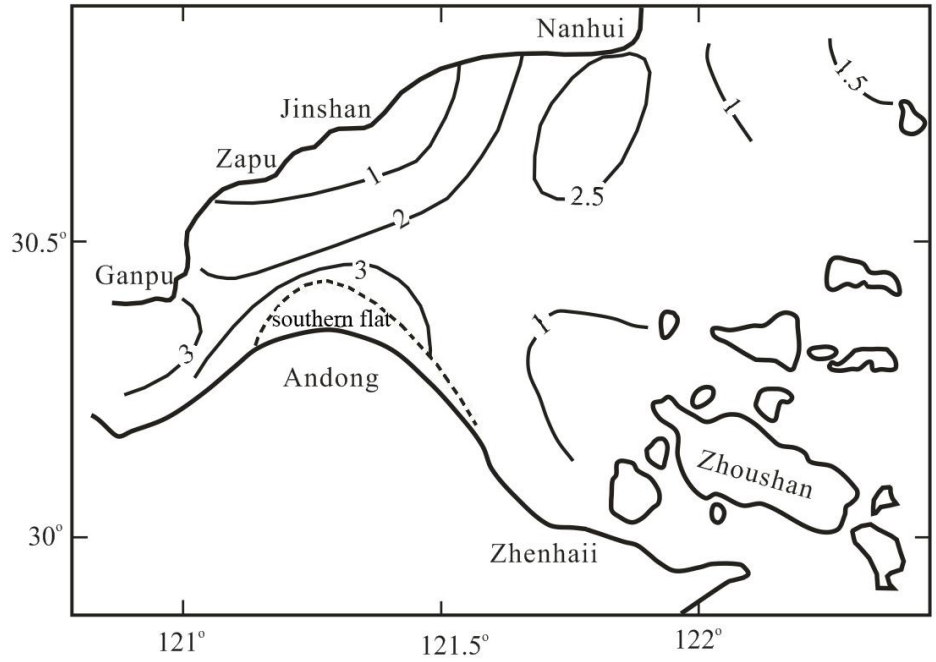

208

209 Fig. 5. Suspended sediment concentration distribution during spring tide in the
210 Hangzhou Bay (modified from Han et al., 2003).

3. Materials and methods

3.1 Collection and analysis of bathymetric data

Due to the strong hydrodynamics and the easily erodible bed, the bed level of the QE changes drastically on seasonal and inter-annual scales. Maximum vertical bed changes can be up to 5 m in a single year (e.g. Chien et al., 1964; Han et al., 2003). Owing to the importance of the morphology for flood protection, navigation, salt water intrusion, etc., there are relatively good historical bathymetric time series available for this reach. In this study, the river channel volumes below mean high-tide level in the QE and the inner bay in the month of April of each year since 1980 were collected to quantify the sediment volume changes.

Available large-scale charts of the Hangzhou Bay mostly only cover the outer Hangzhou Bay or the northern mouth. In this study, detailed and large-scale bathymetric data in the Hangzhou Bay in 1959, 2003, 2010 and 2014, were collected from Zhejiang Surveying Institute of Estuary and Coast (ZSIEC). These data cover the entire bay from the mouth to the Ganpu section. The Odom Hydrotrac echo-sounder was used for the 2003, 2010, 2014 data. The vertical error is 0.1 m, and a global positioning system (GPS) by Trimble was used that gave the positioning error within 1 m. The bathymetric tidal corrections used tidal levels recorded at gauging stations within the area of bathymetric data. Bathymetry in 1959 was surveyed by line echo-sounder, with the vertical error less than 1% for water depths greater than 5m. The positioning errors for the 1959 data were 50 m. The accuracy and quality of the bathymetric data depend on the number and density of elevation points along the traverselines used in the

bathymetry construction. For the latest three depth measurements, the scales of the maps are 1:50,000 at most area, but 1:10,000 locally, including the tidal flats; for the 1959 data, the scale is 1:100,000. These data allowed a detailed analysis of sediment volume changes in the whole bay. As the sediment load from the Changjiang River decreased drastically from 2003 onward, it was possible to determine the bed evolution characteristics of the Hangzhou Bay before and after this date.

The bed elevation in 1959 was mapped with respect to the theoretically lowest astronomical tidal datum at Wusong, whereas the subsequent surveys were with respect to the Chinese National Vertical Datum of 1985. In a first step the bathymetry maps were digitized using ArcGis10.2 software and then normalized to the theoretically lowest astronomical tidal datum at Wusong. Thereafter, the digitized data were transferred from their original projections onto the Beijing 54 coordinates, the bathymetric data being gridded at 100×100 m resolution using the Surfer software package, making use of the kriging interpolation technique (Burrough and McDonnell, 1998), which is appropriate for sparse datasets and has been widely used in previous studies (e.g. Van der Wal and Pye, 2002; Blott, et al., 2006). Subsequently, digital elevation models (DEM) for each digitized bathymetric chart were generated. Spatial deposition and erosion patterns and associated sediment volume changes were calculated by subtraction of the DEMs of different years. The bed level of the reclaimed areas is assumed to be the local average high-tide level, in accordance with the practice of the reclamation procedure. For sediment volume calculations, the bay was divided into three major zones (Fig. 2): the inner Hangzhou Bay upstream of Jinshan (Zone A), the outer, flood-dominated northern Hangzhou Bay where material exchange takes place with the Changjiang Estuary (Zone B), and the outer, ebb-dominated southern

Hangzhou Bay (Zone C).The area of each zone approximately corresponds to 1/3 of the Hangzhou Bay. In addition, for each bathymetric chart, the water depths along four transects were extracted for detailed analysis (Fig. 6).

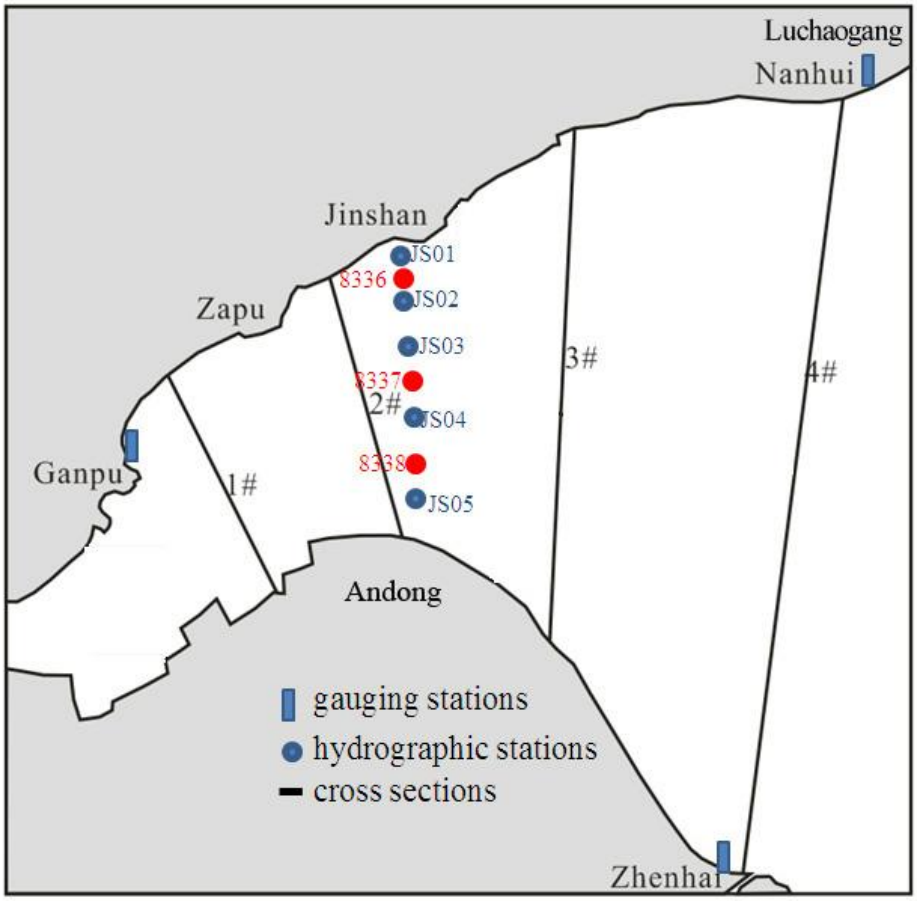

Fig. 6. The cross-sections illustrated in Fig. 8 and the hydrographic stations of 1983 (red cycles) and 2015 (blue cycles).

3.2 Collection and analysis of hydrographic data

Tide levels in the outer Hangzhou Bay and the Changjiang Estuary changed little over the past few decades (Liu et al., 2016), whereas the high-tide level in the inner

Hangzhou Bay increased to a certain extent (Han et al., 2003). Hence, time series of tidal elevation at the Ganpu gauging station since 1950s were collected from Zhejiang Hydrographic Office to determine the annually-averaged tidal elevation and duration changes of rising and falling tides and to analyze the non-linear interaction between hydrodynamics and the morphological evolution over the last decades.

Synchronous hydrographic data along the Jinshan transect, measured in January 1983 and January 2015 was collected. The Jinshan transect is the interface between the inner and outer Hangzhou Bay. The cruise in January 1983 was conducted during the Zhejiang Coast Survey, including 4 hydrographic stations restricted to intermediate tides. At all stations, tidal level, water depth, flow velocity, and SSC were recorded. The flow velocities were recorded by Ekman current meters, and SSCs were determined by taking water samples, which were subsequently filtered through pre-weighed paper filters that were weighed after being oven-dried. All water samples, as well as current measurements, were taken at 1 and 5 m below the water surface and at 1 m above the bottom. The cruise in 2015 included 5 hydrographic stations, including spring, intermediate and neap tide. During the cruise in 2015, the measurements at all stations covered at least a full tidal cycle (25 h). During spring tide the measurements were conducted for 36 h. Flow velocities were recorded by means of an acoustic Doppler current profiler (ADCP) and SSCs were measured hourly at the surface, 0.2H, 0.4H, 0.6H, 0.8H and the bottom, respectively, using an optical backscatter sensor (OBS), where H is the water depth. Meanwhile, the synchronous tide-level data were collected from several tidal gauging stations including Ganpu, Luchaogang and Zhenhai, etc. (Fig. 6).

Water and sediment fluxes were calculated for various tides of each cruise, with water fluxes being the product of the cross-sectional area and mean velocity, and sediment fluxes being the product of water fluxes and SSCs. The fluxes were calculated per layer and then integrated over the vertical profiles for each tidal cycle by summing the hourly data. For cross-sectional area determinations, the representative distance of each station was defined as the sum of the half-distances between the station and its two neighboring stations. If the station was near the coastline, then the shoreward distance was the distance between the station and the coastline. Because the transects ended at the southern and northern banks, the fluxes represent water and sediment entering or leaving the upper Hangzhou Bay. To examine the tidal influences, the relationship between flood-/ebb-averaged fluxes, i.e. the averaged fluxes over the flood and ebb period, and tidal ranges of Luchaogang station were analyzed. The reason for choosing the Luchaogang station is that it is located outside the bay where the tidal range is not influenced by the morphological changes in the Hangzhou Bay, in contrast to the inner Hangzhou Bay where the tidal range has increased, as will be illustrated later.

4. Results

4.1 Morphological evolution of the Hangzhou Bay

Figure 7 illustrates the rates of morphological change in the Hangzhou Bay over successive periods. From 1959-2003, erosion mainly occurred in the northern channel, while deposition occurred in other parts. This pattern is consistent with the earlier reported historical evolution of the Hangzhou Bay that was characterized by “erosion in the north and deposition in the south” (Cao et al., 1985; Han et al., 2003). These

changes were related to large-scale sediment transport induced by the propagation of the tidal wave under the influence of the Coriolis force (ECCHE, 1992). Sediment accumulation during this period was 5.2×10^9 m^3 (Table 1). The sedimentation

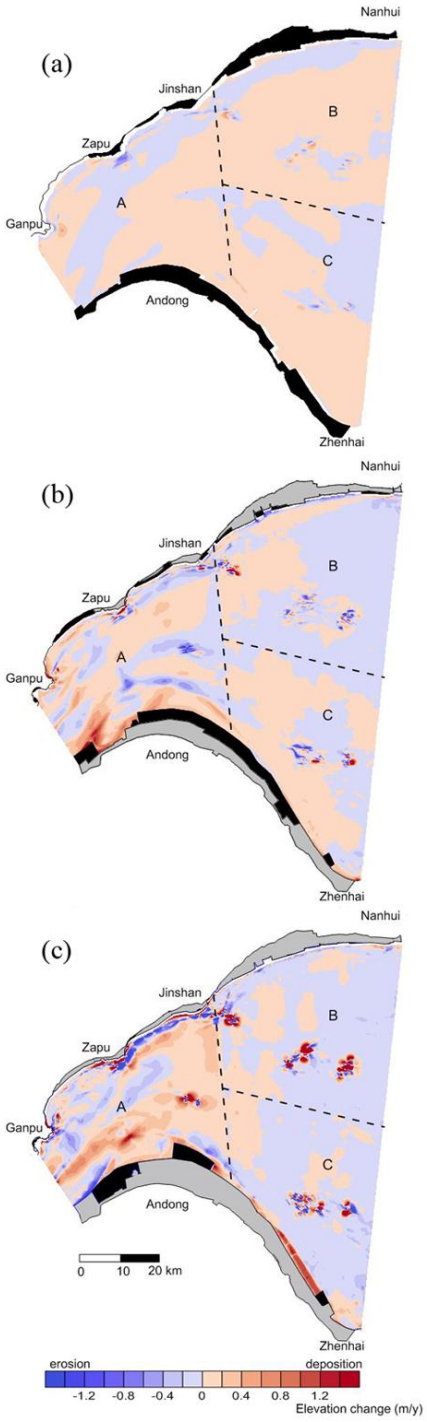

Fig. 7. Rates of morphological change in Hangzhou Bay over successive periods: (a) 1959~2003; (b) 2003~2010; and (c) 2010~2014. The black areas denote land reclamation and the shading areas denote the original shoreline and the latest reclamation.

accumulations in the periods 2003~2010 and 2010~2014 were 1.1×10^9 and 0.6×10^9 m^3, respectively. Correspondingly, the accumulation rates in the three periods were 2.4, 3.3 and 3.0 cm/y, which indicate a generally increasing accumulation trend. Xue (1995) studied volume changes in the Hangzhou Bay using charts of 1887, 1937 and 1987. His results show that the deposition rates in the Hangzhou Bay were 0.8 and 1.5 cm/y in the former and latter 50 years, respectively and the average was 1.15 cm/y for the 100 year period. This suggests that the sedimentation rates in the Hangzhou Bay increased gradually from 1887 to 2014.

All three zones (cf. Fig. 2) showed accumulation in the period 1959~2003. In Zone A (the inner bay) the rate was 2.4 cm/y, and those in zones B and C (the northern and southern parts of the outer bay), were 1.0 and 3.9 cm/y, respectively. In the periods 2003~2010 and 2010~2014, the accumulation rates in Zone A were 9.0 and 13.4 cm/y, revealing a 2.5- and 4.5-fold increase compared to the period 1959~2003. The sediment deposited in the subaqueous area of Zone A since 1959 amounted to 2.36×10^9 m^3, indicating an average bed-level change of about 1.47 m. Zone B switched from accumulation to erosion in the latter two periods, the rates being -4.0 and -1.9 cm/y, respectively. Zone C maintained the accumulating trend from 2003 to 2010, but also switched to erosion from 2010 to 2014, the rates being 5.8 and -1.3 cm/y, respectively.

4.2 Changes in cross-sections

Cross-sections of the inner and outer parts of the bay illustrate the bed-level changes in greater details (Fig. 8). Along cross-sections of the inner bay (1# and 2#), the overall sedimentation can be observed, with the averaged elevations of the sea bed increasing by around 1.5 m. Notable strong sedimentation occurred at the southern bank. The shoreline in the south advanced by about 6 km and 12 km in cross-section 1 and 2#, respectively, since 1959 due to embankment by dyke buildings. The southern flat above mean sea level (MSL) advanced correspondingly and the slope above MSL steepened gradually. Strong sedimentation occurred at the front of the flat (sub-tidal area below MSL) from 1959 to 2003, with the maximum sedimentation of about 5m, indicating a sedimentation rate of about 11 cm/y. The average slopes of the front area of 1 and 2# increased from 1.2‰ to 2.5‰ and from 0.9‰ to 1.7‰, respectively. The steeper slope was more or less maintained during 2003 and 2014. This is probably because the development of the front area of the southern flat is constrained by the main channel of the Hangzhou Bay (Chen et al., 1989). The erosion in the front of 2# between 2003 and 2010 is probably caused by the embankment enhancing the current in the adjacent area.

Along cross-section 3#, the southern channel-shoal system that existed in 1959 disappeared and the bed became smooth. From 1959~2003, the northern part accreted vertically by about 1 m, and the southern shoreline advanced by about 5 km and accreted by about 3.5 m, with the sedimentation rate being about 8 cm/y. After 2003 the bed showed slight accumulation with a maximum of about 0.7 m.

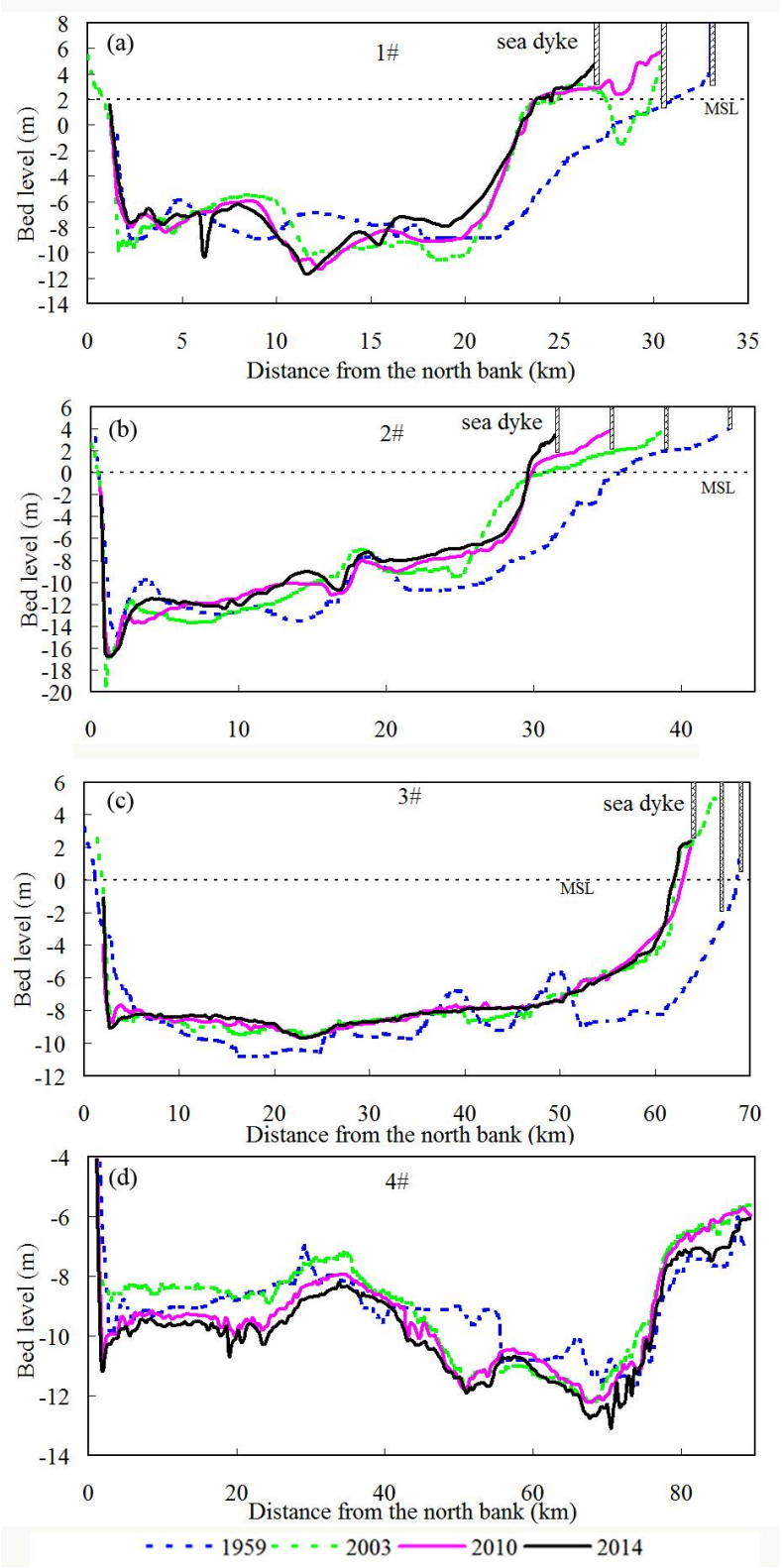

370

371 Fig. 8. Bed level changes along the cross-sections depicted in Fig. 6.

Cross-section 4#, located at the bay mouth, showed accumulation in the northern and southern parts, but erosion in the central part in the period from 1959~2003, on average amounting to about 1 m. From 2003-2010 the most remarkable change was the up to 1 m erosion at the northern mouth. From 2010-2014 the whole section along the mouth eroded about 0.4 m.

4.3 Morphological evolution of the Hangzhou Bay-Qiantang Estuary system

There are strong water and sediment exchanges between the Hangzhou Bay and the QE (e.g. Chen et al., 1990; Han et al., 2003). In the last decades, the bed change in the QE was characterized by continuous accumulation, which was mainly caused by artificial coastal embankments since the 1960s, which resulted in constriction of the estuary (Li and Dai, 1986; Han et al., 2003; Pan et al., 2010).

Figure 9 illustrates time series of channel volumes below the mean high-tide level of the QE and the inner bay since 1980. Channel volume decreases indicate accumulation. Before 1993, the volume in the QE was basically stable, fluctuating around an average of about 4.1×10^9 m^3. From 1993~2005, the volume continuously decreased with the rate of 71×10^6 m^3/y, and the accumulate rate being 10.2 cm/y. The fluctuation of volumes between neighboring years should be attributed to the variation of the water discharge from Qiantang River. The bed level change in the QE is sensitive to the river discharge because the fine sediment in the estuary can be easily resuspended. The seabed of the QE tends to be eroded during high flow season or years, and deposited during low flow season or years (Chien et al., 1964; Han et al., 2003; Yu et al., 2012). After 2006, a new relatively stable volume reached with an average channel volume of 3.0×10^9 m^3. For the

inner bay, the bathymetric data was deficient before 1986. Since 1986, the volume decreased stepwise in two stages. From 1986~2005, the average volume change was about 74×10^6 m^3/y, whereas since 2006 it doubled to about 150×10^6 m^3/y (Fig. 9). Correspondingly, the accumulation rates were 4.4 cm/y and 9.0 cm/y, respectively. It is interesting to note that the difference between the average volume changes before and after 2006 (76×10^6 m^3) was almost identical to that of the QE in the period from 1993~2005. This suggests that, when the morphological evolution of the QE was relatively stable, the location of sediment deposition moved seaward to the inner Hangzhou Bay. The total accumulation rate of the two areas together remained more or less constant.

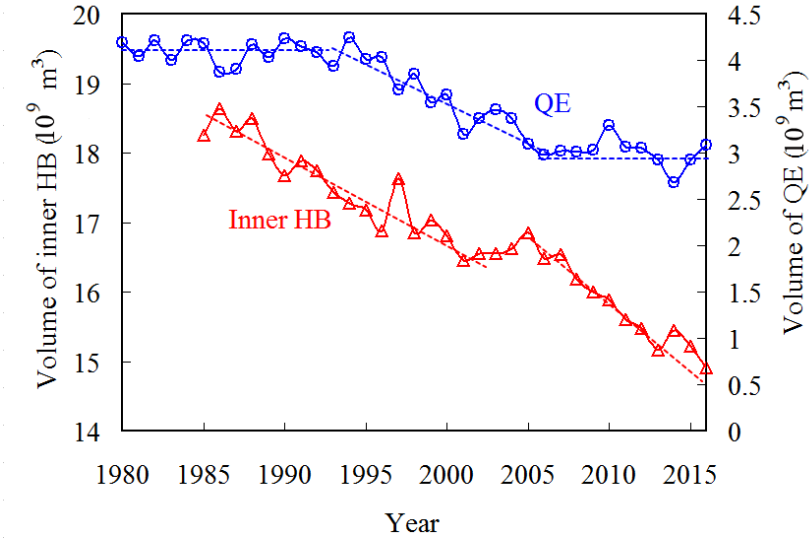

Fig. 9. Temporal changes in channel volumes below mean high-tide level in the Qiantang Estuary and the inner Hangzhou Bay (zone A in Fig.2).

Table 2 lists the channel volume changes of the QE and the Hangzhou Bay in the same periods. The accumulation rates were 6.4, 9.8 and 8.4 cm/y, from 1959~2003, 2003~2010 and 2010~2014, respectively. For the Hangzhou Bay-QE system, the

accumulation rates in the three periods were 2.9, 4.2 and 3.8 cm/y, respectively. It is obvious that, although the sediment load from the Changjiang River drastically decreased in recent years, the deposition rate in the system did not decrease but actually increased to a certain extent.

4.4 Feedback of morphological evolution on hydrodynamics

Hydrodynamics, sediment transport and bed evolution generally interact in nonlinear fashion (e.g. Dronkers, 1986; Hibma et al., 2003; Yu et al., 2012; Winterwerp and Wang, 2013). The asymmetry of the tide is one of the controlling factors for residual sediment transport and hence morphological evolution of estuaries and tidal basins (e.g. Aubrey, 1986; Dronkers, 1986; Friedrichs and Aubrey, 1988; Wang et al., 2002). In estuaries, the tide is flood-dominant if the flood duration is shorter than the ebb duration, and ebb-dominant if the opposite is true (Wang et al., 2002).

Figure 10a and 8b illustrates the time series of annually averaged high- and low-tide levels and the tidal ranges, respectively, at the Ganpu gauging station. Since the 1970s, the high-tide level has increased gradually from around 4.7 m to 5.4 m, whereas the low-tide level remained stable around -2.6 m up to 2000 before increasing gradually to -2.4 m since then. In accordance, the annually-averaged tidal range increased by about 0.6 m since the 1970s. The increasing high-tide level is caused by the land boundary changes due to the coastal embankment which enhanced the tidal wave reflection (Xie et al., 2005). A good relationship exists between the embanked area and the annual high level (Fig. 11). An addition factor for the high tidal level increase is the increasing

436 occurrence of storm surges in the Hangzhou Bay area (Liu et al., 2016). The change in
437 the low-tide level was mainly related to the changes in bed level (Han et al., 2003).
438
439 Figure 10c illustrates the annually-averaged flood and ebb durations based on the water
440 level data at the Ganpu station. As can be seen, the duration of the flood is shorter than
441 that of the ebb. Before 1980, the flood duration was around 5 h 30 min and the ebb
442 duration around 6 h 50 min, the ratio between the two being constant around 0.85. Since
443 1981, the duration of the flood became gradually shorter, whereas that of the ebb
444 became gradually longer. From 1981 to 2015, the change in duration of both flood and
445 ebb was about 40 minutes. Subsequently, the ratio between the two gradually decreased
446 to 0.63. This reveals that the flood dominance of the inner Hangzhou Bay became
447 enhanced due to coastal embankment and sediment accumulation.
448
449 Figure 12 illustrates the relationships between the water and sediment fluxes across the
450 Jinshan transect and the tidal range at the Luchaogang gauging station at the time of the
451 cruises in 1983 and 2015. As can be seen, both water and sediment fluxes correlate well
452 with the tidal range. At a mean tidal range of 3.2 m, the water fluxes in 1983 and 2015
453 were 108×10^8 m^3 and 80×10^8 m^3, respectively, indicating that the gross water flux
454 decreased by about 25% over the last 30 years (Fig. 12a). The decrease in the tidal
455 prism is related to the decreasing tidal flat (e.g. Van der Wal et al., 2002; Winterwerp
456 and Wang, 2013). However, the sediment fluxes remained similar over the same period.
457 At the mean tidal range of 3.2 m, the sediment flux in the two reference years was
458 1.45×10^6 t.

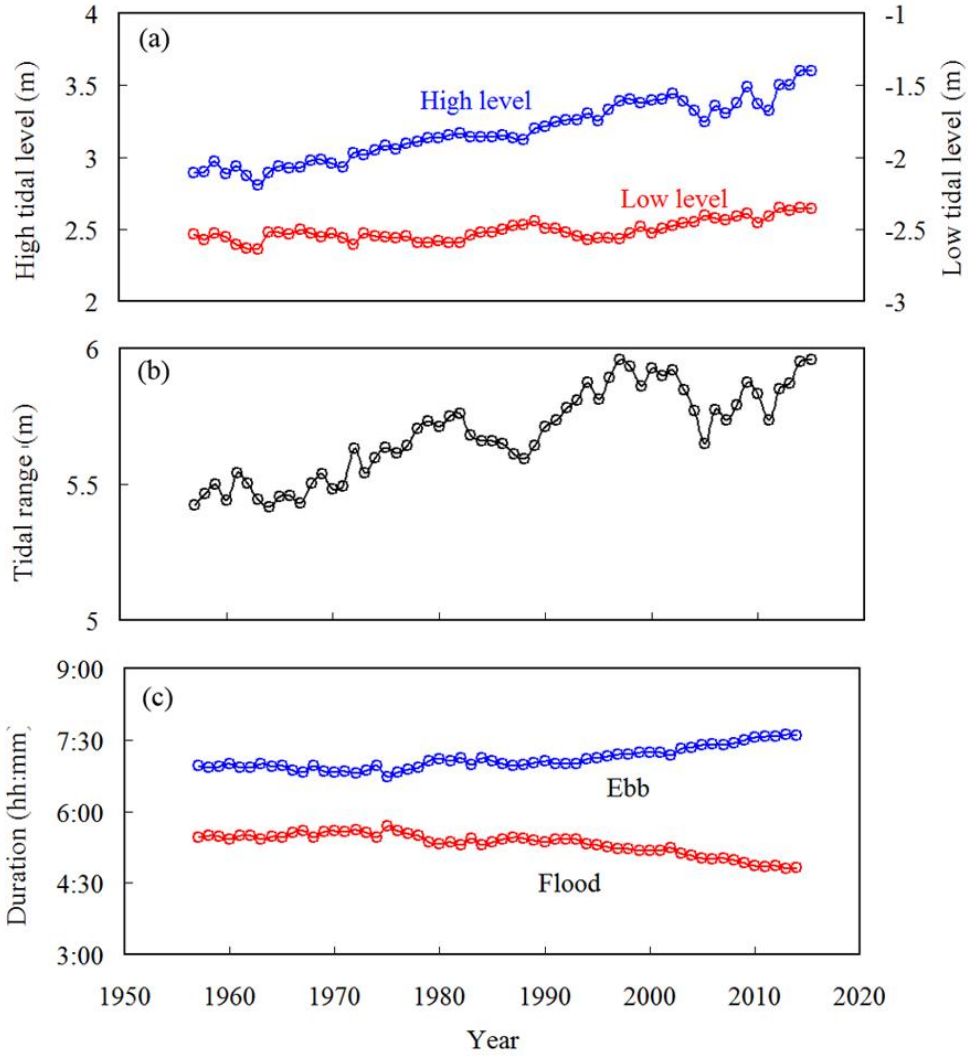

459

460 Fig. 10. Annually-averaged high- and low-tide levels (a), tidal range (b) and flood/ebb

461 durations at the Ganpu gauging station. (data from Zhejiang Hydrographic Office).

462

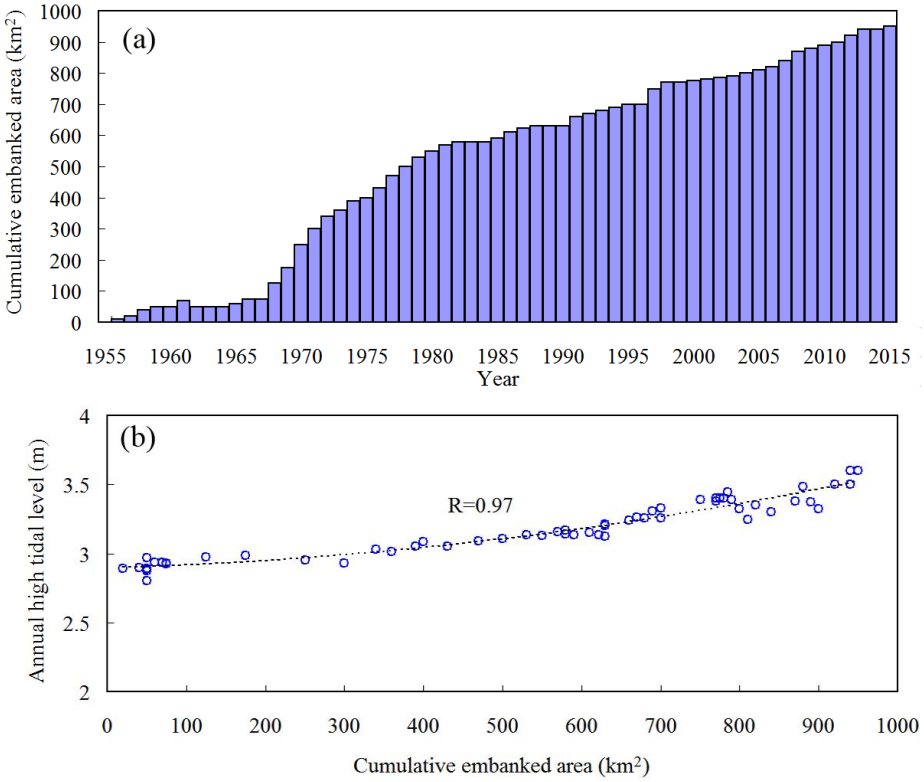

463

464 Fig. 11. Time series of the cumulative embanked area in the Qiantang – Hangzhou Bay
465 area (a) and the relationship between the cumulative embanked area and the annual high
466 tidal level at Ganpu station (b). Data in panel (a) is from Tang and Cao (2016).

467

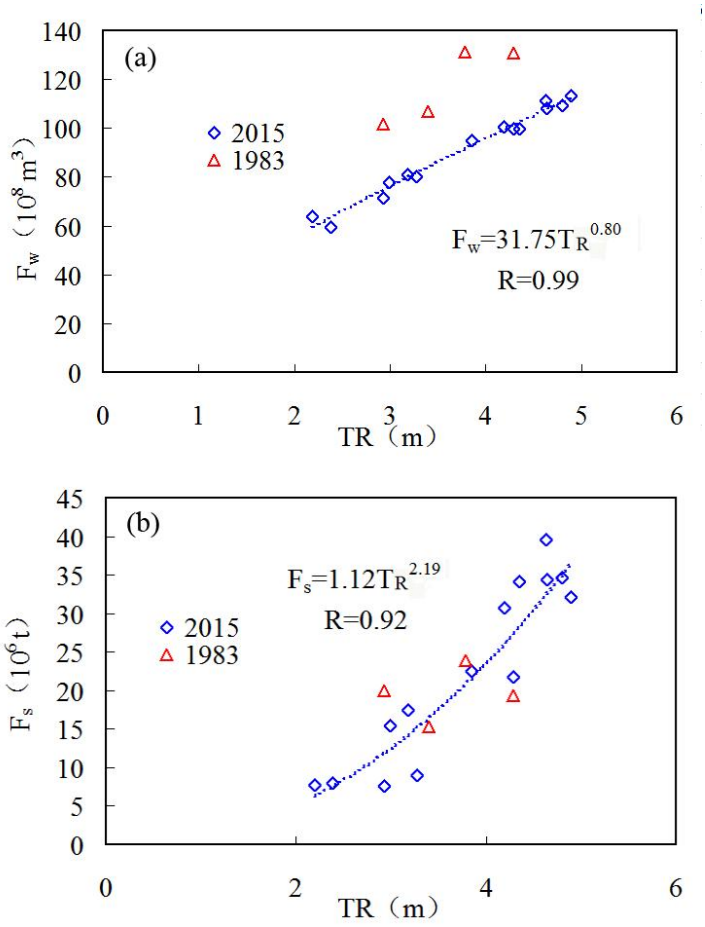

468

469 Fig. 12. The relationships between flood/ebb-averaged water fluxes (F_w) (a) and
470 sediment fluxes (F_s) (b) across the Jinshan transect versus the tidal range at the
471 Luchaogang station (T_R) during the winter cruises of 1983 and 2015.

472

473 Because sediment flux is a function of water flux and suspended sediment
474 concentration, it is obvious that the SSC increased in recent years. This is related to the
475 stronger tidal currents caused by the narrowed cross-section. However, in comparison to
476 the water fluxes, the net sediment flux is very small, being the difference between the
477 very large flood and ebb fluxes, and is therefore extremely difficult to measure or
478 compute with any degree of confidence (Townend, 2005). Given that the sediment flux
479 has not changed, but that the flood dominance has been enhanced over the last 30 years,

it is reasonable to assume that, at present, more sediment is transported landward in one tidal cycle. This explains the increasing accumulation rate in the inner Hangzhou Bay.

5. Discussion

5.1 Influence of the decreasing sediment load from the Changjiang River

The sediments in the Hangzhou Bay and the Qiantang Estuary are mainly derived from the Changjiang River (e.g. Su and Wang, 1989; Chen et al., 1990). After the river-borne sediments enter the Changjiang Estuary, about one-half is deposited within the estuary, most of the other half being dispersed to the south, the remainder northward to the Jiangsu coastal sea (Chen et al., 1985; Milliman et al., 1985). The reduction of the Changjiang sediment load caused wide concern of what influence this would have on sediment delivery to the Hangzhou Bay and the associated morphological development.

The results of the present analysis show that, in recent years, the sedimentation rates in the Hangzhou Bay and the QE as a whole has not decreased, but rather increased to some extent, as shown in Fig.7 and Table 2. This can be attributed to the adjustment of the area of the outer Changjiang Estuary. The reduction of the sediment load from the Changjiang River is mainly related to the flood season from June to September (e.g. Dai et al., 2016; Xie et al., 2017). Recent research showed that in the outer Changjiang estuary, the SSC has not decreased in the flood seasons of the last few decades (Xie et al., 2017). During the last 7000 years of the post-glacial transgression, the large amounts of sediment from the Changjiang formed an elongated, up to 50 m thick mud belt that stretches from the Changjiang Estuary almost up to Taiwan (Liu et al., 2007). The tides in this region play an important role in sediment transport. Large tidal ranges

and strong tidal currents, in combination with shallow water depths, small seabed slopes and little wave action, have resulted in active resuspension of fine-grained sediment from the local seabed (Gao et al., 2015).

As pointed out by Kennedy (1984), estuaries trap significant quantities of material and thus act as filters between land and the oceans. The principal sediment supply of the Hangzhou Bay is neither from the Qiantang River nor directly from the Changjiang River. Instead, there are two filters, i.e. the Changjiang Estuary and the mud area in the outer Changjiang Estuary. The drastic reduction in the sediment load of the Changjiang River would thus initially be recorded in two buffer areas. This can be supported by the recent study of Yang et al (2011) and Luo et al (2017) who found that the Changjiang subaqueous delta is experiencing overall net erosion since the construction of the Three Gorges Dam in 2003 and suggested that the delta recession will continue to occur in the near future because the Changjiang sediment discharge will further decrease in the near future due to the construction of new dams. On the other hand, recent hydrological surveys revealed that the annually-averaged net sediment flux into the Hangzhou Bay has decreased slightly by about 10% after 2003 (Xie et al., 2017), whereas the net sediment fluxes in the coastal area south of Zhoushan islands have not detected to be decreased apparently in last decades (Deng et al., 2017). The slight decrease sediment supply at the mouth of the bay caused the erosion in the outer bay in recent years (Fig. 7b and c). Its influence on the inner bay and the QE has been overcome by the coastal embankment, because the sediment in the inner bay and the QE comes from the outer bay (Chen et al., 1990). This phenomenon agrees with the long-term morphodynamic model by Yu et al (2012) that with the sediment supply decrease at the seaside of the

estuary, erosion will firstly observed at the mouth area. The morphological effects on the inner bay and the QE are expected to lag behind by a relatively longer time.

5.2 Morphological development of the southern flat

Tidal flats are important geomorphological units in estuarine and coastal environments, which provide habitat for wild lifes, resources for land reclamation and protection against extreme storm events, and play an important role in global carbon cycling and climate change (e.g. Allen and Pye, 1992; Yang et al., 2005; De Vriend et al., 2011; Friedrichs, 2011). The accreting southern tidal flat in the Hangzhou Bay plays as a sink for sediment from Changjiang Estuary under the role of the secondary plume of Changjiang Estuary, also for the sediment output from the QE during high river flow season or years (Li and Xie, 1993). In the last centuries, the flat advanced fast with the average rate of about 25 m/y and vertical sedimentation rate of about 5 cm/y, under natural condition (Chen et al., 1990).

The strong sedimentation of the southern flat is related to the large-scale flow patterns in the Hangzhou Bay. The northern bay is dominated by flood currents while the southern bay is dominated by ebb currents (e.g. Cao et al., 1985; Su and Wang, 1989; Xie et al., 2009). Ebb currents diverge at the front of the southern flat due to the increasing cross-sectional width. Subsequently, the sediment transport capacity of ebb currents decreased, and strong sedimentations occur (Cao et al., 1985; Han et al., 2003). Because the embankments in the last decades have been mainly carried out above MSL, the changes of large-scale flow patterns has been limited (Shao, 2016). In addition, SSCs in the front of tidal flat area is high, with the vertically averaged SSC usually

above 3 kg/m^3 (Fig. 5). The sedimentation rate of the southern flat has been increased apparently in the last decades, compared to the above-mentioned rate of about 5 cm/y in natural conditions (Fig. 8). This is probably related to the increasing SSC in the front area. Recent study of Van Maren et al (2016) revealed that land reclamations in estuaries will lead to an increase in SSC because of the decrease in accommodation space for fine-gained sediments. This can also be evaluated from the fact that despite the water fluxes into the inner bay have decreased apparently since 1980s, the sediment fluxes can be more or less maintained (Fig. 12).

The cross-sectional profiles of the accretion-dominated tidal flat are normally convex (Fig. 8), similar to other accretional intertidal flats in the world (Kirby, 2000; Yang et al., 2005; Friedrichs, 2011; Wang et al., 2014). Apparent reductions in width of the southern flat, due to coastal embankments by building sea dykes, have resulted in steeper fronts. This is similar to the observations in the Changjiang Estuary and Jiangsu coast (Yang et al., 2005; Van Maren et al., 2013; Wang et al., 2014). Wind waves can cause erosion on the wide intertidal flat (Kirby, 2000; Yang et al., 2005; Wang et al., 2014). The reduction in the intertidal flat width can cause a concentration of wave energy on the lower flat and in the sub-tidal area, with relative deep water, resulting in bed erosion (Wang et al., 2014). A model applied to the accreting intertidal flat shows that tidal flats with abundant sediment supply can persistently prograde with the similar slope, remaining in the equilibrium shape under natural conditions (Liu et al., 2010). However, southern flat in the Hangzhou Bay is not the case. The font area of the flat has become progressively steeper because of the constraint by the main channel of the bay.

5.3 Morphological response model of the Hangzhou Bay

577 Over the last decades, the annual tidal levels in the outer Changjiang Estuary and in the
578 Hangzhou Bay have fluctuated around their multi-year averages. Hence the influence of
579 sea-level rise on sediment transport and morphological evolution of the Hangzhou Bay
580 have been minor. The main channel of the QE used to meander continuously, and the
581 coastal wall revetments used to collapse frequently, resulting in serious economic losses
582 and even losses of human lives, besides making the development of resources such as
583 navigation channel maintenance difficult. Since the 1960s, large-scale coastal
584 embankments in the QE have been carried out for the purpose of flood defense, urban
585 land requirements, etc. (Li and Dai, 1986; Han et al., 2003; Pan et al., 2010).
586 Embankments occurred gradually over time (Fig. 3a and 7), having to date resulted in
587 more than 1000 km^2 of reclaimed tidal flats. In the process, the estuarine width was
588 greatly reduced, for example from about 10 km to 2.5 km at Yanguan and from about
589 22 km to18 km at Ganpu.
590
591 The morphological response in the QE is related to progressive coastal embankment.
592 Before 2006, the QE and the inner Hangzhou Bay showed sediment accretion (Fig. 9).
593 The accumulation in the QE needed sediment supply from downstream (i.e. the inner
594 Hangzhou Bay). After 2006, when the morphological evolution in the QE has been
595 basically stable, accumulation shifted downstream. As a consequence, the accumulation
596 rate in the inner Hangzhou Bay increased (Fig. 7 and 9), the sediment source being the
597 outer Hangzhou Bay. This is consistent with Chen et al (1990), who showed, based on
598 sedimentological analysis, that the sediment in the QE comes mainly from the
599 Hangzhou Bay, whereas the sediment in the inner Hangzhou Bay derives mainly from

600 the outer bay. Overall, the sediment accretion in the Hangzhou Bay and the QE is
601 characterized by the gradually seaward shifting trend.
602
603 Worldwide, land reclamation and dredging have been, and still are, common practice in
604 many estuaries, many researchers reporting increased sedimentation as a consequence
605 (e.g. Inglish and Kestner, 1958; Sherwood et al., 1990; Pye and French, 1993; Van der
606 Wal et al., 2002). This can mainly be attributed to enhancement of flood dominance due
607 to decrease tidal flat area (Van der Spek, 1997). In the viewpoint of the estuarine
608 convergence, stronger convergence results in the large longitudinal sandbar in the QE
609 shifts seaward (Yu et al., 2012). The increasing sedimentations in the Hangzhou Bay-
610 QE system in last decades observed in this study agree with their numerical model
611 results.
612
613 In response, the northern bay-mouth switched from a depositional mode to an erosional
614 mode in recent years. This is in agreement with previous observation by Dai et al
615 (2014). Besides the above-mentioned causes, there are probably several other factors.
616 First, there are probably direct sediment exchanges between the northern bay mouth and
617 southern CE mouth across the front of the Nanhui shoal (Su and Wang, 1989; Chen et
618 al., 1990). With the reduction of the Changjiang sediment load, the progradation rates of
619 tidal flats along the CE slowed down or even reversed to erosion (Yang et al., 2005;
620 Van Maren et al., 2013; Wang et al., 2015). Hence the SSC in the outer CE has
621 decreased by about 20-30% after the Three Gorges Dam construction in 2003 (Li et al.,
622 2012; Xie et al., 2017). The SSC decrease of the outer CE would decrease the direct
623 sediment supply to the northern Hangzhou Bay. On the other hand, more than 150 km^2

along the Nanhui shore of the northern mouth has been reclaimed since the 1980s (Fig. 3b). The reclamation intercepted large amounts of sediment, which could be originally transported into the northern Hangzhou Bay. On the other hand, the eastward propagation of the Nanhui flat by about 10 km in recent years has increased the distance and changed the route by which Changjiang sediment can enter the Hangzhou Bay (Fig. 3b).

5.4 Future morphological evolution trends

Progressive land reclamation in coastal environments continually change the circumjacent hydrodynamics and sediment transport (e.g. Van der Spek, 1997; Van der Wal., et al., 2002; Wang et al., 2015). During the last decades, both the annually-averaged high and low tidal levels in the inner bay have been increased due to shoreline constriction and sediment accumulation. The annually-averaged durations of rising and falling tides have been shorten and lengthened, respectively, indicating that the flood dominance in the inner bay has been enhanced (Fig. 10). As a result, the net landward sediment flux over one tidal cycle at the interface between the inner and outer bay has been increased to some extent (Fig. 12). In return, this nonlinear feedback mechanism has promoted the sediment accumulation in the inner bay.

At present, the large-scale coastal embankments in the QE have continuously increased the constriction of the estuary over several decades. In the near future, only some local areas will be reclaimed (Pan et al., 2010). However, the sediment accumulation will not cease synchronously due to the enhanced flood-dominance and landward sediment transport. The temporal scales of estuarine morphodynamics are related to the spatial

scales involved (De Vriend, 1996). The larger the spatial scale is, the longer the time that would be needed for the morphological adjustment. In view of the large spatial scale of the Hangzhou Bay and the complex sediment transport behavior, the timescale for morphological readjustment in the Hangzhou Bay is expected to be in the order of several decades. The accumulation trend of the inner bay will continue for some time, while erosion of the outer bay will also continue in order to supply sediment to the inner part.

6. Conclusions

Although the sediment load from the Changjiang River has reduced, especially since 2003 when the Three Gorges Dam was constructed and operated, the sedimentation rate in the adjacent Hangzhou Bay has not decreased as expected. The outer Changjiang Estuary acts as a buffer area and sediment sources for the Hangzhou Bay. Besides other reasons, such as land reclamation in the Qiantang and Changjiang estuaries, the documented erosion in the northern Hangzhou Bay can be partly attributed to the drastic reduction of the Changjiang sediment load because that part directly exchanges sediment with the Changjiang Estuary.

The large-scale human interventions played an important role in the morphological evolution of the Hangzhou Bay-Qiantang Estuary system. The coastal embankment increased the estuarine constriction and, to a certain extent, enhanced the flood dominance in the inner part. Subsequently, the sedimentation rate in the estuary increased. The morphological changes have been related mainly to the implementation process of the coastal embankment. With progressive seaward coastal embankment, sediment accumulation has resulted in gradual seaward aggradation. The annually-

673 averaged high and low tidal levels in the inner bay have been increased and the flood
674 dominance in the inner bay has been enhanced apparently. The tidal prism at the
675 interface between the inner and outer bay has decreased by about 25% since 1980s,
676 while the net landward sediment flux has been intensified to a certain extent. The
677 enhancing flood dominance and landward sediment transport are responsible for the
678 increasing sedimentation in the estuary. Furthermore, stronger sedimentations have
679 occurred at the southern shoreline, and the upper and sub-tidal flat has been steeper due
680 to coastal embankments and the constraint of the main channel of the bay. Although the
681 coastal embankment will cease in the near future, the morphological response is
682 expected to continue on for a longer time.
683

684 **Acknowledgements**

685 This research was supported by the National Natural Science Foundation of China
686 (grant number 41676085, 51379190); Zhejiang Provincial Natural Science Foundation
687 of China (grant number LY16D060004). We wish to thank two anonymous reviewers
688 for their constructive comments to improve this work greatly. We also thank Mr.
689 Chengfei Hu for his help in the preparation of the figures.
690

691 **References**

692 Allen, J.R.L., Pye, K., 1992. Coastal saltmarshes: their nature and importance. In: Allen,
693 J.R.L., Pye, K. (Eds.), Saltmarshes, Morphodynamics, Conservation and Engineering
694 Significance. Cambridge Uni. Press, Cambridge, U.K, pp. 1-18.
695 Aubrey, D.G., 1986. Hydrodynamic controls on sediment transport in well-mixed bays
696 and estuaries. In: Van de Kreeke, J. (Ed.), Physics of Shallow Estuaries and Bays.
697 Lecture Notes on Coastal and Estuarine Studies Vol. 16. Springer-Verlag, Berlin, pp.
698 245–276.

699 Blott, S.J., Pye, K., Van der Wal, D., Neal, A., 2006. Long-term morphological change
700 and its causes in the Mersey Estuary, NW England. Geomorphology 81(1-2), 185–206.
701 Burrough, P.A. McDonnell, R.A., 1998. Principles of Geographical Information
702 Systems. Oxford University Press, Oxford, UK, 352 pp.
703 Cao, P.K., Gu, G.C., Dong, Y.F., Hu, F.X., 1985. Basic characteristics of sediment
704 transport in Hangzhou Bay. J. East China Normal Uni., (3), 75-84 (in Chinese with
705 English abstract).
706 Chen, J.Y., Wang, B.C., Yu, Z.Y., 1989. Developments and Evolution of China's Coast.
707 Shanghai Sci. Tech. Pub., Shanghai, 556 pp (in Chinese).
708 Chen, J.Y., Zhu, H.F., Dong, Y.F., Sun J.M., 1985. Development of the Changjiang
709 Estuary and its submerged delta, Cont. Shelf Res. 4, 47-56.
710 Chien, N., Sie, H. S., Chow, C. T., Lee, Q.P., 1964. The fluvial processes of the big
711 sand bar inside the Chien Tang Chiang Estuary. Acta Geograph. Sin., 30(2), 124-142 (in
712 Chinese with English abstract).
713 Dai, Z.J., Fagherazzi, S., Mei, X.F., Gao, J.J., 2016. Decline in suspended sediment
714 concentration delivered by the Changjiang (Yangtze) River into the East China Sea
715 between 1956 and 2013. Geomorphology 268, 123–132.
716 Dai, Z.J., Liu, J.T., Xie, H.L. Shi W.Y., 2014. Sedimentation in the Outer Hangzhou
717 Bay, China: the influence of Changjiang sediment load. J. Coast. Res. 30, 1218–1225.
718 Deng, B., Wu, H., Yang, S.L., Zhang, J., 2017. Longshore suspended sediment transport
719 and its implications for submarine erosion off the Yangtze River Estuary. Estuarine
720 Coastal Shelf Sci. 190, 1-10.
721 De Vriend, H.J., 1996. Mathematical modelling of meso-tidal barrier island coasts. Part
722 I: Emperical and semi-emperical models, In: Liu, P.L.F. (Ed.), Advances in Coastal
723 Ocean Engineering. World Scientific, Singapore, pp. 115-149.
724 De Vriend, H.J., Wang, Z.B., Ysebaert, T., Herman, P.M.J., Ding, P.X., 2011. Eco-
725 Morphological Problems in the Yangtze Estuary and the Western Scheldt. Wetlands,
726 31(6), 1033-1042.
727 Dronkers, J., 1986. Tidal asymmetry and estuarine morphology. Nether. J. Sea. Res. 20
728 (2/3), 117–131.
729 Dyer, K.R., 1997. Estuaries - physical introduction, 2nd ed. John Wiley and Sons,
730 Chichester. 195 pp.

731 Editorial Committee for Chinese Harbors and Embayment (ECCHE), 1992. Chinese
732 Harbors and Embayment (Part V).. China Ocean Press, Beijing. 357pp (in Chinese).
733 Eisma, D., 1998. Intertidal deposits: river mouth, tidal flats, and coastal lagoons. CRC
734 Press, Boca Raton. 495pp.
735 Fan, D.D., Tu, J.B., Shang, S., Cai, G.F., 2014. Characteristics of tidal-bore deposits
736 and facies associations in the Qiantang Estuary, China. Mar. Geol. 348, 1-14.
737 Fairbridge, R.W., 1980. The estuary: its definition and geodynamic cycle. In: Olausson,
738 E., Cato, I. (Eds.), Chemistry and Biogeochemistry of Estuaries. John Wiley & Sons,
739 New York, NY, pp. 1-36.
740 Friedrichs, C.T., 2011. Tidal flat morphodynamics: a synthesis. In: Hansom, J.D. and
741 Flemming, B.W. (eds), Treatise on estuarine and coastal science, vo.3: Estuarine and
742 coastal geology and geomorphology. Elsevier, pp. 34.
743 Friedrichs, C.T., Aubrey, D.G., 1988. Non-linear tidal distortion in shallow well-mixed
744 estuaries: a synthesis. Estu. Coast Shelf Sci. 27, 521-45.
745 Gao, S., Wang, Y.P., 2008. Material fluxes from the Changjiang River and their
746 implications on the adjoining continental shelf ecosystem. Cont. Shelf Res. 28, 1490-
747 1500.
748 Gao, S., Wang, D.D., Yang, Y., Zhou, L., Zhao, Y.Y., GAO, W.H., Han, Z. C., YU, Q.,
749 Han, Z.C., Dai, Z.H., Li, G.B., 2003. Regulation and Exploitation of Qiantang Estuary.
750 China Water Power Press, Beijing, 554pp (in Chinese).
751 Hibma, A., Stive, M.J.F., Wang, Z.B., 2004. Estuarine morphodynamics. Coast. Eng.
752 51, 765-778.
753 Inglish, C.C., Kestner, F.J.T., 1958. The long-term effects of training walls,
754 reclamation, and dredging on estuaries. Proc. Institution Civil Eng. 9, 193–216.
755 Kirby, R., 2000. Practical implications of tidal flat shape. Cont. Shelf Res. 20, 1061-
756 1077.
757 Kennedy, V. S., 1984. The estuary as a filter. Academic Press, New York. 511pp.
758 Lane, A., 2004. Bathymetric evolution of the Mersey Estuary, UK, 1906-1997: causes
759 and effects. Estu. Coast. Shelf Sci. 59, 249–263.
760 Li, G.B., Dai, Z.H., 1986. Fluvial processes and reclamation of the Qiantang Estuary.
761 Inter. J. Sed. Res. 1(1), 56–66.

762 Li, P., Yang, S.L., Milliman, J.D., Xu, K.H., Qin, W.H., Wu, C.S. , Chen, Y.P. , Shi,
763 B.W., 2012. Spatial, temporal, and human-induced variations in suspended sediment
764 concentration in the surface waters of the Yangtze Estuary and adjacent coastal areas.
765 Estu. Coast. 35, 1316–1327.
766 Li, Y., Xie, Q.C., 1993. Dynamical development of the Andong tidal flat in Hangzhou
767 Bay, China. Donghai Mar. Sci. 11(2), 25-33 (in Chinese with English abstract).
768 Liu, J.P., Xu, K.H., Li, A.C., Milliman, J.D., Velozzi, D.M., Xiao, S.B., Yang, Z.S.,
769 2007. Flux and fate of Yangtze River sediment delivered to the East China Sea.
770 Geomorphology 85(3-4), 208–224.
771 Liu, X.J., Gao, S., Wang, Y.P., 2011. Modeling profile shape evolution for accreting
772 tidal flats composed of mud and sand: A case study of the central Jiangsu coast, China.
773 Cont. Shelf Res. 31(16): 1750-1760
774 Liu, Y.F., Xia, X.M., Chen, S.L., Cai, T.L., 2016. Morphological evolution of Jinshan
775 Trough in Hangzhou Bay (China) from 1960 to 2011, Estuar. Coast. Shelf Sci. In press.
776 Luo, X.X., Yang, S.L., Wang, R.S., Zhang, C.Y., Li, P., 2017. New evidence of
777 Yangtze delta recession after closing of the Three Gorges Dam. Sci. Rep. 7, 41735.
778 Milliman, J.D., 1997. Blessed dams or damned dams, Nature 386, 325–326.
779 Milliman, J.D., Farnsworth, K.L., 2011. River discharge to the coastal ocean—A global
780 synthesis. Cambridge Uni. Press, Cambridge, UK. 394pp.
781 Milliman, J.D., Shen, H.T., Yang, Z.S., Robert, H.M., 1985. Transport and deposited of
782 river sediment in the Changjiang estuary and adjacent continental shelf. Cont. Shelf
783 Res. 4, 37-45.
784 Pan, C.H., Shi, Y.B., Han, Z.C., 2010. Regulation of Qiantang River estuary and
785 scientific and technological innovations. China Water Resour. 14, 13–16 (in Chinese
786 with English abstract).
787 Pye, K., French, P.W., 1993. Erosion and accretion processes on British Saltmarshes,
788 Vol. 5. Cambridge Environ. Res. Cons., Cambridge.
789 Shao, M.M., 2016. Impacts of reclamation of tidal dynamics in Hangzhou Bay. M.Sc.
790 thesis, Zhejiang University.
791 Sherwood, C.R., Jay, D.A., Harvey, R.B., Hamilton, P., Simenstad, C.A., 1990.
792 Historical changes in the Columbia river estuary. Prog. Oceanogr. 25, 299–352.

Su, J.L., Wang, K.S., 1989. Changjiang River plume and suspended sediment transport in Hangzhou Bay. Cont. Shelf Res. 9(1), 93–111.

Syvitski, J.P.M., Vörösmarty, C.J., Kettner, A.J., Green, P., 2005. Impact of humans on the flux of terrestrial sediment to the global coastal ocean. Science 308(15), 376–380.

Tang, Z.W., Cao, Y., 2016. Beach resources evolution and trend analysis of Qiantang River estuary section under the condition of Narrowing river. Zhejiang Hydrotec., (2): 20-23.

Townend, I., 2005. An examination of empirical stability relationships for UK estuaries. J. Coast. Res. 21, 1042–1053.

Townend, I., Whitehead, P., 2003. A preliminary net sediment budget for the Humber Estuary. Sci. Total Environ. 314–316, 755–767.

Trenhaile, A.S., 1997. Coastal Dynamics and Landforms. Clarendon, Oxford, UK. 382pp.

Van der Spek, A.J.F., 1997. Tidal asymmetry and long-term evolution of Holocene tidal basins in The Netherlands: simulation of palaeo-tides in the Schelde estuary. Mar. Geol. 141, 71–90.

Van der Wal, D., Pye, K., Neal, A., 2002. Long-term morphological change in the Ribble Estuary, northwest England. Mar. Geol. 189, 249–266.

Van der Wal, D., Pye, K., 2002. The use of historical bathymetric charts to assess morphological and sediment budget change in estuaries. Geogr. J. 169(1), 21–31.

Van Maren, D.S., Yang, S.L., He, Q., 2013. The impact of silt trapping in large reservoirs on downstream morphology: the Yangtze River. Ocean Dyn. 63, 691–707.

Van Maren, D.S., Oost, A.P., Wang, Z.B., Vos, P.C., 2016. The effect of land reclamations and sediment extraction on the suspended sediment concentration in the Ems Estuary. Mar. Geol. 376, 147-157.

Wang, Y.P., Gao, S., Jia J.J., Thompson, C.E.L., Gao, J.H., Yang, Y., 2012. Sediment transport over an accretional intertidal flat with influences of reclamation,Jiangsu coast, China. Mar. Geol. 291-294, 147-161.

Wang, Z.B., Jeuken, M.C.J.L., Gerritsen, H., De Vriend, H.J., Kornman, B.A., 2002. Morphology and asymmetry of the vertical tide in the Wester-Schelde estuary. Cont. Shelf. Res. 22, 2599–2609.

824 Wang, Z.B., Van Maren, D.S., Ding, P.X., Yang, S.L., Van Prooijen, B.C., De Vet,
825 P.L.M., Winterwerp, J.C., De Vriend, H.J., Stive, M.J.F., He, Q., 2015. Human impacts
826 on morphodynamic thresholds in estuarine systems. Cont. Shelf Res. 111, 174–183.
827 Whitehouse, R.J.S., 2002. Predicting estuary morphology and process: an assessment of
828 tools used to support estuary management. In: Editor (ED.), Proc. Seventh Inter. Conf.
829 on Estu. Coast. Model., St. Petersburg, Florida, USA, 2001, pp. 344–363.
830 Winterwerp, J.C., Wang, Z.B., 2013. Man-induced regime shifts in small estuaries – I:
831 theory. Ocean Dyn. 63(11), 1279–1292.
832 Xie, D.F., Pan, C.H., Wu, X.G., Gao, S., Wang, Z.B., 2017. The variations of sediment
833 transport patterns in the outer Changjiang Estuary and Hangzhou Bay over the last 30
834 years. J. Geophy. Res. Ocean, 122, doi:10.1002/2016JC012264.
835 Xie, D.F., Gao, S., Wang, Z.B., De Vriend, H.J., 2009. Numerical modeling of tidal
836 currents, sediment transport and morphological evolution in Hangzhou Bay, China.
837 Cont. Shelf. Res. 28, 316–328.
838 Xue, H.C., 1995. Deposition character of Changjiang estuary in the past 100 years. In:
839 Editor (Ed.), Proc. 17th Symposium on Coastal Engineering. Publisher, Beijing (in
840 Chinese).
841 Xie, Y.L., Huang, S.C., Wang, R.F., Zhao, X., 2005. Numerical simulation of effects of
842 reclamation in Qiantang Estuary on storm surge at Hangzhou Bay. Ocean Eng. 25(3),
843 61-67 (in Chinese with English abstract).
844 Yang, S.L., Zhang, J., Zhu, J., Smith, J.P., Dai, S.B., Gao, A., Li, P., 2005. Impact of
845 dams on Yangtze River sediment supply to the sea and delta intertidal wetland response.
846 J. Geophy. Res. 110, F03006.
847 Yang, S.L., Milliman, J.D., Li, P., Xu, K., 2011. 50, 000 dams later: erosion of the
848 Yangtze River and its delta. Glob. Planet. Change 75(1-2), 14–20.
849 Yu, J., Cao, Y., 2006. Sediment deposition after regulation and reclaiming of Qiantang
850 Estuary. J. Sed. Res. (1), 17–24 (in Chinese with English abstract).
851 Yu, Q., Wang, Y., Gao, S., Flemming, B., 2012. Modeling the formation of a sand bar
852 within a large funnel-shaped, tide-dominated estuary: Qiantangjiang Estuary, China.
853 Mar. Geol. 299–302, 63–76.
854

855 Table 1. Accumulation and erosion in Hangzhou Bay in different periods.

Time interval	Volume changes (10^6 m^3)				Accumulation rate (cm/y)			
	Zone A	Zone B	Zone C	Hangzhou Bay	Zone A	Zone B	Zone C	Hangzhou Bay
1887~1937				1800				0.8 a
1937-1987				3700				1.5 a
1959~2003	1715	724	2729	5168	2.4	1.0	3.9	2.4
2003~2010	952	-466	606	1092	9.0	-4.0	5.8	3.3
2010~2014	771	-126	-75	571	13.4	-1.9	-1.3	3.0

856 *Positive values denote sediment accumulation while negative values denote sediment
857 erosion. The same below.
858 [a] Based on the data from Xue (1995).
859

860 Table 2. Net accumulation in the Hangzhou Bay-Qiantang Estuary system in different
861 time intervals.

Time intervals	Hangzhou Bay		Qiantang Estuary		Hangzhou Bay-Qiantang Estuary system	
	VC	AR	VC	AR	VC	AR
1959~2003	5168	2.4	1916	6.4	7084	2.9
2003~2010	1092	3.3	477	9.8	1569	4.2
2010~2014	571	3.1	231	8.4	802	3.8

862 *VC: volume changes, in 10^6 m^3; AR: accumulation rate, in cm/y.
863

Figure Captions

Fig. 1. Temporal variations of annual water and sediment discharges measured at the Datong gauging station located at the tidal limit 640 km upstream from the Changjiang River mouth (data from the Changjiang River Hydraulic Engineering Committee).

Fig. 2. Locations in Hangzhou Bay referred to in the text. The dashed lines depict water depths. The definitions of the three zones referred to in the statistics of Tables 1 are also given.

Fig. 3. Coastal embankment in the Qiantang Estuary (a) and land reclamations in front of the Nanhui flat bordering the Changjiang Estuary (b).

Fig. 4. Surface sediment grain size in Hangzhou Bay (from Xie et al., 2009).

Fig. 5. Suspended sediment concentration distribution during spring tide in the Hangzhou Bay (modified from Han et al., 2003).

Fig. 6. The cross-sections illustrated in Fig. 8 and the hydrographic stations of 1983 (red cycles) and 2015 (blue cycles).

Fig. 7. Rates of morphological change in Hangzhou Bay over successive periods: (a) 1959~2003; (b) 2003~2010; and (c) 2010~2014. The black areas denote land reclamation and the shading areas denote the original shoreline and the latest reclamation.

Fig. 8. Bed level changes along the cross-sections depicted in Fig. 6.

Fig. 9. Temporal changes in channel volumes below mean high-tide level in the Qiantang Estuary and the inner Hangzhou Bay (zone A in Fig.2).

885 Fig. 10. Annually-averaged high- and low-tide levels (a), tidal range (b) and flood/ebb
886 durations at the Ganpu gauging station. (data from Zhejiang Hydrographic Office).

887 Fig. 11. Time series of the cumulative embanked area in the Qiantang – Hangzhou Bay
888 area (a) and the relationship between the cumulative embanked area and the annual high
889 tidal level at Ganpu station (b). Data in panel (a) is from Tang and Cao (2016).

890 Fig. 12. The relationships between flood/ebb-averaged water fluxes (F_w) (a) and
891 sediment fluxes (F_s) (b) across the Jinshan transect versus the tidal range at the
892 Luchaogang station (T_R) during the winter cruises of 1983 and 2015.

893